

Al₂O₃ referenced microring resonators for the detection of interleukin-6

Ward Hendriks
Integrated Optical Systems
University of Twente
Enschede, The Netherlands
w.a.p.m.hendriks@utwente.nl

Meinder Dijkstra
Integrated Optical Systems
University of Twente
Enschede, The Netherlands
m.dijkstra@utwente.nl

Jeroen Kortेरik
Integrated Optical Systems
University of Twente
Enschede, The Netherlands
j.p.kortेरik@utwente.nl

¹ Sonia García Blanco
Integrated Optical Systems
University of Twente
Enschede, The Netherlands
s.m.garciablanc@utwente.nl

Abstract—Concentrations down to 300 pM of the interleukin-6 biomarker, identified as an inflammatory marker for severe COVID-19 infection, have been detected in buffer using referenced microring resonators in the emerging Al₂O₃ integrated photonic platform. Antifouling was achieved by applying an Xantec HC1000M hydrogel.

Keywords— Sensing, COVID-19, Interleukin-6, biomarker, microring resonator.

I. INTRODUCTION

Severely ill patients with COVID-19 tend to have high concentrations of pro-inflammatory cytokines such as interleukin-6 (IL-6)[1], [2]. In addition, for patients receiving organ support in ICU, treatment with IL-6 receptor antagonists has been reported to improve outcomes, including survival[3]. Therefore, facilitating monitoring of the IL-6 biomarker is of interest for treatment optimization and possibly early detection of severe inflammation. Biosensors based on the microring resonator technology can lead to portable multiplexed point-of-care devices, facilitating physicians in diagnosis and treatment. Here, we present the measurement of IL-6 biomarker in buffer using referenced microring resonators in the Al₂O₃ integrated photonics platform with a Xantec HC1000M hydrogel[4] antifouling layer. First the sensor design and fabrication are discussed followed by the functionalization and sensing protocol. Finally, the measurement results and obtained limit of detection (LOD) are discussed.

II. SENSOR DESIGN

The performance of a microring resonator interrogated by tracking the position of the resonances by scanning a tunable laser is dictated by the LOD of the system,

$$LOD = \frac{3\sigma}{S} \quad (1)$$

where σ is the standard deviation of the Lorentzian resonance position and S is the sensitivity to refractive index variations in the sensing medium. An optimal sensor is therefore obtained when the sensitivity is maximized and the noise minimized. The total noise in the system is composed of the uncertainty of the model fit to determine the resonance position, the temperature induced variance of the resonance position and the wavelength

repeatability of the laser. The fit uncertainty can be shown to scale with the FWHM, the sample rate over the resonance and the signal to noise ratio[5]. The fit uncertainty is in the order a few femtometer as expected by the Cramer Rao lower bound. The low thermo-optic coefficient of Al₂O₃, measured to be $1.1 \cdot 10^{-5}$ RIU/K, results in a measured temperature sensitivity of 7 pm/K for the chosen waveguide geometry and TM operation. Combined with a sample stage temperature variation of ~ 1 mK, a temperature induced noise of a few femtometer should be considered. Finally, the laser repeatability of the Agilent 81600B/200 system used is 0.2 pm, which cannot be improved. The waveguide dimensions are chosen to maximize the sensitivity and minimize the LOD at a layer thickness around 500 nm and a waveguide width of 2200 nm. The waveguide width is chosen to minimize sidewall overlap for a minimal FWHM of the resonance. In order to further minimize the effect of wavelength repeatability on the noise as well as to reduce the influence of bulk refractive index and non-specific binding, a second non-functionalized ring with a slightly different free spectral range (FSR) is used as reference.

III. METHODS

Al₂O₃ layers with a thickness at the center of the wafer of 550 nm are deposited by reactive sputtering, at a substrate set temperature of 700 °C and at a target compound fraction of 2%, on 10 cm diameter silicon wafers with an 8 μm oxide layer. The layer thickness decreases down to 500 nm at the outer edge of the wafer. After sputtering, the wafer is coated with a negative resist (AR-N 7520) and a conductive coating (AR-PC 5090), allowing for electron beam lithography (Raith EBPG5150) to write the waveguides layouts. Next the pattern is developed and the waveguides etched using chemically assisted reactive ion etching (Oxford PlasmaPro 100 Cobra). The resist is stripped, followed by the deposition of PECVD oxide(Oxford 80) using a stainless-steel shadow mask to keep the sensing windows open. For improved adherence of the hydrogel, a 10 nm SiO₂ layer is deposited on the sensing region. The entire chip surface is covered with the hydrogel.

Selective functionalization of the sensor ring is achieved using a PDMS flow channel over the sensor ring and not over the reference ring. Prior to the functionalization, DI water is flown for 5 minutes followed by a Xantec elution buffer for 5 minutes

and DI for 15 minutes. The chip is then activated for binding by a flow of 100 mM EDC in an MES/NHS buffer solution for 15 minutes followed by DI water for 5 minutes. For the functionalization, an acetate buffer with pH 4.5 and 5 $\mu\text{g/ml}$ IL-6 antibody (Biolegend 501101, 21 kDa) is flown for 30 minutes followed by 30 minutes of DI water. As a deactivation step, a Xantec quenching buffer is flown for 15 minutes followed by 5 minutes of DI water. Finally in order to remove any unbound antibody, an elution buffer is flown for 5 minutes followed by 6 minutes of DI water. After functionalization, the PDMS channel is removed and replaced by a channel covering both the sensor and reference rings. Then increasing concentrations of IL-6 antigen (Biolegend 570802) in 10 mM PBS are flown over both rings for 90 minutes per concentration preceded by 30 minutes of PBS flow (Figure 1).

IV. RESULTS

The resonance spectra obtained every ~ 9 seconds contain the resonances of both the reference and sensor ring resonators. Given the design of the FSR of both rings, two maximally separated resonances are assured within the 10 nm scan range and chosen to fit using an Lorentzian line shape with the Matlab nonlinear least squares algorithm. The difference of the resonance positions of both rings is extracted for the consecutive flows of PBS and analyte and shown in Figure 1a. While the flows are consecutive in time, the sensorgrams are displayed overlaid for easy comparison. The referencing of both rings significantly removes bulk index shifts and temperature drift from the sensorgram. For large shifts, a residual shift remains as can be seen at the 20 minute mark when switching from PBS to analyte. This is a consequence of the fabrication tolerances resulting in non-equal sensitivity of both rings. In addition the rings are separated by 1 mm allowing for variance in the local environment. The referencing also reduces the laser repeatability noise from ~ 0.2 pm, as specified for the laser system, to a standard deviation determined to be ~ 0.05 pm over 70 minutes. With the designed sensitivity of the sensor of ~ 150 nm/RIU, a LOD of $\sim 10^{-7}$ RIU is obtained for the sensor. The detection limit for the biosensing experiment is defined as the total resonance shift over the 90 minute analyte flow, shown in Figure 1b, that exceeds the 3σ band shown in Figure 1c. For the concentration of 300 pM this is clearly achieved while the 75 pM measurement is below the detection limit. In this experiment, the time is taken from the start of the flow as in Figure 1a, meaning that the detection limit is exceeded after 30 minutes of analyte flow for the 300 pM concentration. In addition, the order of magnitude difference in slope indicates that the detection limit is lower than the shown 300 pM. The total shift as shown in Figure 1b starts to saturate for the concentration of 20 nM likely indicating a dynamic range constrained below μM concentrations.

V. CONCLUSIONS

Referenced microring resonator biosensors in Al_2O_3 with Xantec HC1000M hydrogel constitute a promising platform for low concentration biomarker sensing. A robust surface functionalization protocol for the selective functionalization of

the sensor and reference ring is demonstrated. The label-free detection of 300 pM of the IL-6 protein, associated with severe cases of COVID-19, was demonstrated in PBS. While this detection limit is still two orders of magnitude away from clinically relevant values for COVID-19[6], several improvement opportunities exist, such as the improvement of the laser repeatability and the optimization of the functionalization protocol and affinity of the antibody-protein pairs. Finally, the detection limit is in the range of clinically relevant values for cytokine release syndrome making the results presented here a promising first step towards point-of-care detection of cytokines in an acute care setting.

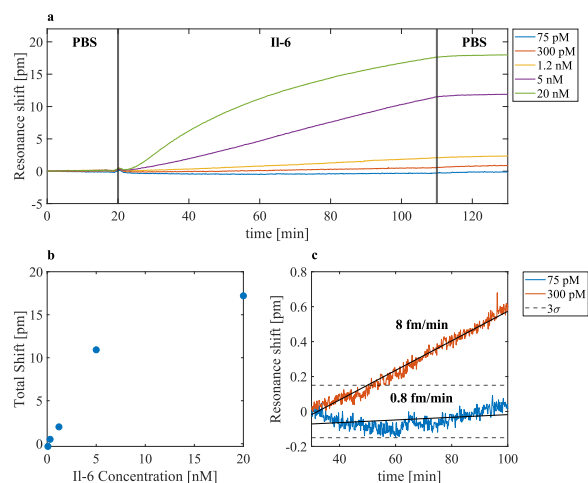


Figure 1 a. Sensorgram of consecutive flows of IL-6 concentrations in PBS buffer. b, Total resonance shift after 90 minutes of IL-6 flow at different concentrations. c, Comparison of the 75 pM and 300 pM response, the first and last 10 minutes of the analyte flow are excluded to make sure liquid switching deviations as seen at 20 minutes in figure a do not influence the analysis.

VI. ACKNOWLEDGMENTS

The authors thank Erk Gedig from Xantec Bioanalytics and Jan Hendriks for their advice in the development of the functionalization and measurement protocol.

REFERENCES

- [1] Y. Tang, J. Liu, D. Zhang, Z. Xu, J. Ji, and C. Wen, 'Cytokine Storm in COVID-19: The Current Evidence and Treatment Strategies', *Frontiers in Immunology*, vol. 11. Frontiers Media S.A., p. 1708, Jul. 10, 2020, doi: 10.3389/fimmu.2020.01708.
- [2] S. Hojyo *et al.*, 'How COVID-19 induces cytokine storm with high mortality', *Inflammation and Regeneration*, vol. 40, no. 1. BioMed Central Ltd, Oct. 01, 2020, doi: 10.1186/s41232-020-00146-3.
- [3] 'Interleukin-6 Receptor Antagonists in Critically Ill Patients with Covid-19', *N. Engl. J. Med.*, vol. 384, no. 16, pp. 1491–1502, Feb. 2021, doi: 10.1056/nejmoa2100433.
- [4] 'XanTec bioanalytics GmbH | Sensors and surfaces'. <https://www.xantec.com/> (accessed Aug. 18, 2021).
- [5] M. R. Foreman, W.-L. Jin, and F. Vollmer, 'Optimizing detection limits in whispering gallery mode biosensing', *Opt. Express*, vol. 22, no. 5, p. 5491, Mar. 2014, doi: 10.1364/OE.22.005491.
- [6] D. E. Leisman *et al.*, 'Cytokine elevation in severe and critical COVID-19: a rapid systematic review, meta-analysis, and comparison with other inflammatory syndromes', *Lancet Respir. Med.*, vol. 8, no. 12, pp. 1233–1244, Dec. 2020, doi: 10.1016/S2213-2600(20)30404-5.